Enhancing throughput of disorder-based broadband spectrometer using correlated disorder

Bhupesh Kumar, Sebastian Schulz

Bhupesh Kumar, Sebastian A. Schulz, "Enhancing throughput of disorder-based broadband spectrometer using correlated disorder," Proc. SPIE 12334, Emerging Applications in Silicon Photonics III, 1233408 (11 January 2023); doi: 10.1117/12.2645034

Event: SPIE Photonex, 2022, Birmingham, United Kingdom

Enhancing Throughput of Disorder based Broadband Spectrometer using Correlated Disorder

Bhupesh Kumar[a] and Sebastian A. Schulz[a,*]

[a] SUPA, School of Physics and Astronomy, University of St. Andrews, Fife, KY16 9SS, UK

ABSTRACT

We performed numerical simulation and fabrication of a compact and sensitive high-resolution spectrometer, by superimposing controlled disorder on a photonic crystal. This simultaneously creates an in-plane speckle and suppresses out-of-plane scattering. We perform two- dimensional and three- dimensional numerical simulations to demonstrate reduced out-of-plane scattering and enhanced throughput in such disorder-enhanced photonic crystal structures compared to completely disorder structures without any compromise on resolution.

Keywords: Spectrometer, Silicon Photonics, Correlated Disorder, Multiple scattering

1. INTRODUCTION

Optical Spectrometers are a highly important instrument to be used for a wide range of applications such as chemical and biological sensing,[1] environmental monitoring,[2] optical communication[3] or light source characterization. Traditional bench top grating-based spectrometers are typically designed by using bulky dispersive optics, large detector arrays and long optical path lengths. Such spectrometers can achieve high resolution and bandwidth but with high cost and bulky design. Miniaturization of the spectrometers down to sub-millimeter scale could enable low-cost spectroscopy for wide range of application, including lab-on-a-chip functionality, in-situ or in-vitro characterization system. In recent time various schemes such as Echelle grating,[4,5] arrayed waveguide grating[6,7] and microelectro mechanical systems (MEMS) technology combined with fourier transform infrared spectroscopy has been used to realize compact on-chip spectrometers.[8–10] To reduce the size of a spectrometer, one needs to increase the effective path length while maintaining a small footprint. Recently, disordered scattering based spectrometer have emerged to enable broadband optical operation.[11–13] Their working principle is based on the use of multiple scattering of light in a random structure to create a wavelength sensitive speckle patterns. Generated speckle patterns are stored in a calibrated transmission matrix. This transmission matrix contain spectral-to-spatial mapping of the spectrometer. After calibration any of the input spectrum can be reconstructed by measuring its intensity pattern at the output and its inverse multiplication with the transmission matrix. However, current disorder-based speckle spectrometers have prohibitively high optical losses - the majority of light is scattered out-of-plane, and never reaches the detection region,[13] resulting in poor efficiency and signal to noise ratios. To overcome this issue, we propose to superimpose controlled disorder on a photonic crystal to enhanced the wavelength separation region that creates an in-plane speckle and simultaneously suppresses out-of-plane scattering,[14–16] leading to compact and sensitive high-resolution spectrometers.

2. NUMERICAL SIMULATION OF DISORDER SPECTROMETER

Fig.1(a) shows the geometry of the disorder spectrometer. We choose semicircular disk of diameter = 50 μm as a scattering region. Scattering region consists of randomly distributed arrays of identical air holes of diameter 150 nm. Air holes cover 15 % of the total scattering area. To reduce the loss due to back scattering from the base of the semicircle, we placed a photonic crystal layer having a band gap in the spectral region of interest. A defect line was created in the middle of photonic crystal layer to inject the input signal into the scattering region. We choose four scattering configurations: uniform random distribution, periodic distribution with a lattice constant of 300 nm and periodic disorder configurations with ± 15 nm and ± 45 nm deviation from a lattice point.

Further author information: (Send correspondence to S. A. S)
A S.A.S.: E-mail: sas35@st-andrews.ac.uk,

Emerging Applications in Silicon Photonics III, edited by Callum G. Littlejohns, Marc Sorel,
Proc. of SPIE Vol. 12334, 1233408 · © 2023 SPIE · 0277-786X
doi: 10.1117/12.2645034

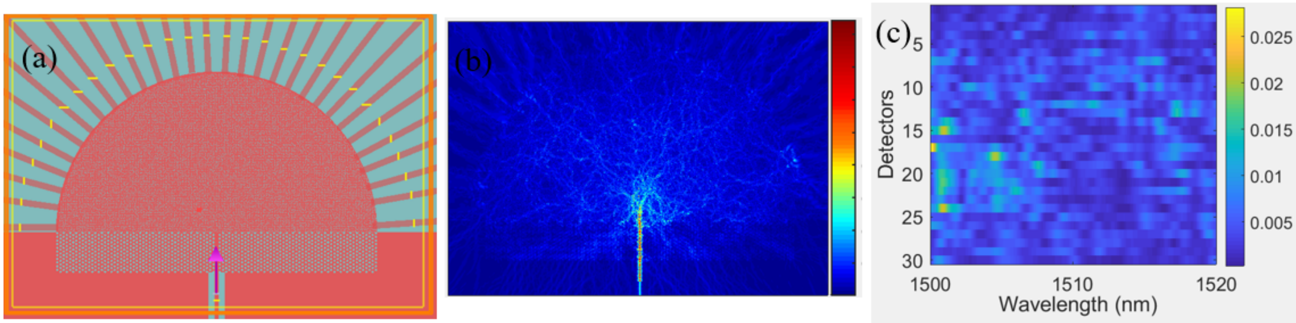

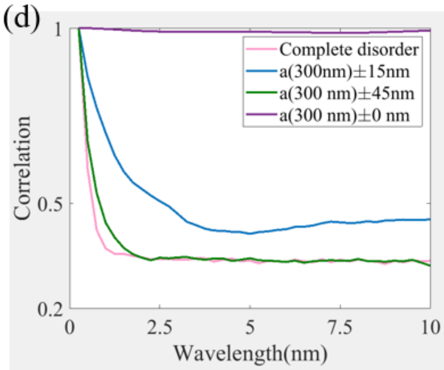

(e)

Scatterer Configuration	HWHM (nm)
Disorder	0.6
a± 45 nm	0.7
a± 15 nm	2.7
a± 0 nm	∞

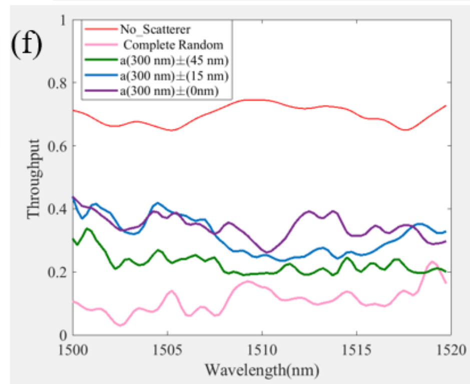

Figure 1. (a) Schematic of the disorder spectrometer layout considered for 2D numerical simulations (b) Numerical 2D FDTD (Lumerical) simulation of the TE polarized light intensity diffusing through controlled disorder medium at wavelength(λ) =1500 nm. (c) Transmission martix calibrated near IR wavelength from 1500 nm to 1520 nm for periodic disorder configuration with a deviation of ± 45 nm in a lattice period of 300 nm. (d) Correlation function for each scattering configuration. (d) Table showing HWHM for each of the four scattering configuration. (e) Integrated throughput for all four configuration as a function of wavelength. Top red plot is the reference throughput for the case when there is no scattering element in semicircular region.

Incoming light injected via waveguide defect after multiple scattering reaches 30 readouts waveguides each with a base width of 1 μm. We record wavelength-dependent intensity distribution for a NIR wavelength range of 1500-1520 nm at a step size of 0.25 nm in each case in a matrix called transmission matrix. Fig.1(c) shows Transmission matrix for the case of periodic disorder with a deviation of ± 45 nm from lattice point. To measure the spectral resolution of the different scattering configurations. We calculate the half-width-half-maximum (HWHM) of the correlation function(fig.1(d)) for all four configurations .Table in fig.1(c) compare HWHM of the all four scattering configuration. We also measure the throughput for all the configuration by integrating the intensity collected across each detector waveguide. For all periodic and periodic disorder configuration we found more throughput compare to complete disorder configuration. with almost comparable spectral resolution. 2D numerical simulations confirm that periodic disorder configuration provides more throughput compare to complete disorder configuration with almost comparable resolution.

To confirm further, we also performed 3D numerical FDTD (Lumerical) simulations to calculate out-of-plane scattering. We use same disorder configurations as used in experiment with identical FF of 15 %. To reduce numerical simulation time we choose a smaller semicircle of radius 10 μm. Fig.2(a) and 2(b) shows in-plane and out-of-plane intensity distribution respectively at a wavelength(λ)= 1500 nm. Fig. 2(c) compare integrated out-of-plane scattering for TE polarized light in wavelength(λ) range 1500-1520 nm. For almost identical spectral resolution, combination of disorder and periodicity enhance throughput by 30 % compared to complete disorder configuration for the same scatterer density.

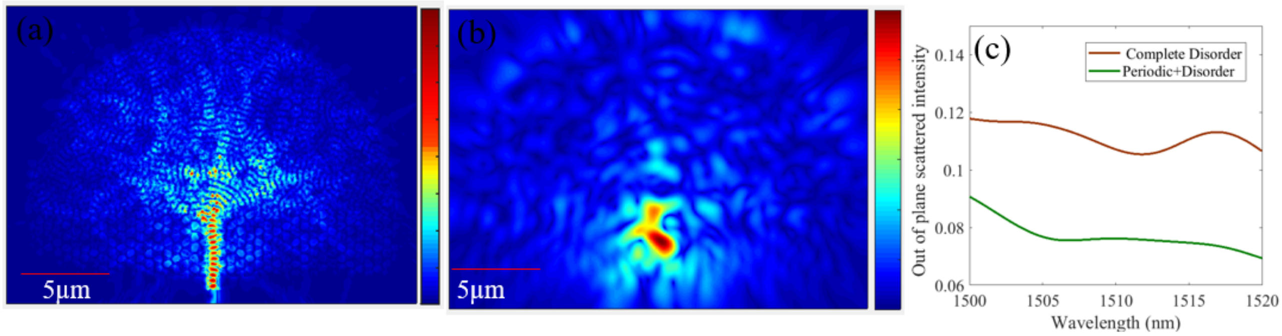

Figure 2. (a) Numerical 3D FDTD (Lumerical) simulation of the TE polarized light intensity diffusing through controlled disorder medium at wavelength(λ) =1500 nm. (b) Simulated out-of-plane scattered light intensity collected at a distance of 500 nm above the top surface at wavelength(λ)= 1500 nm. (C) Comparison of out-of- plane scattered light integrated over sample surface for a wavelength(λ) range of 1500-1520 nm.

3. DEVICE FABRICATION AND CHARACTERIZATION

We fabricate two different disorder configurations on a Silicon on Insulator (SOI) wafer using electron beam lithography. For the first case, scatterers (air holes, Diameter= 150 nm) are distributed as a disordered periodic lattice of period 300 nm with a position disorder of ± 45 nm for each lattice point in the x-y plane. For the second case, scatterers are distributed randomly (Uniform probability distribution). The scatterer are distributed in a semi-circular area of radius 25 μm, occupying in total 15 % of the semi-circular area in both cases. A photonic crystal (PhC) layer with a complete bandgap in the wavelength region of interest (1500-1525 nm) is fabricated at the base to avoid light loss due to back reflection.

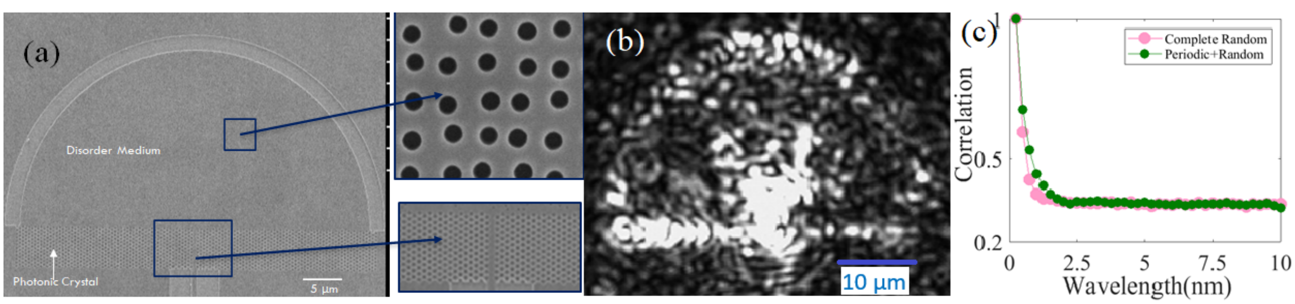

Figure 3. (a) Scanning electron microscope image of the fabricated device on a Silicon on Insulator (SOI) wafer using electron beam lithography. Scatterers (air holes, Diameter= 150 nm) are distributed as a disordered aperiodic lattice in a semicircular area of radius 25 μm, occupying in total 15 % of the total surface area. A Photonic crystal mirror is fabricated at the base to avoid light loss due to back reflection. A semicircular groove in the outer region of the scattering area is used to collect light for detection. (b) Experimental image of the speckle pattern generated by CW laser light at = 1520 nm. Out of plane scattered light at the edge of semicircle is used for detection.(C) Normalized spectral correlation function plotted for a wavelength range of 1500-1510 nm, complete random: HWHM= 0.70 nm, periodic disorder: HWHM = 0.80 nm.

A defect waveguide in the centre of the PhC allows the incoming light to couple into the spectrometer. A semi-circular air groove in the outer region of the scattering area is used to collect light for detection. A continuous tunable laser (TS-100, EXFO) is used to characterize the fabricated devices. Laser light was coupled to the input waveguide by fiber coupling and light scattered from the outer semicircle air groove is imaged using an InGaAs camera (Raptor, Owl 640 II). Image of the out-of-plane scattered light recorded at λ= 1500 nm for the periodic disorder configuration is shown in fig.3(b). The intensity distributed across the outer circumference is divided into 125 equal sections each acting as independent detector. The intensity distribution was recorded across the 10 nm bandwidth from 1500-1510 nm with a step size of 0.25 nm and is stored in a transmission matrix which later can be used to identify the input wavelength.[13] To determine the resolution of the spectrometer a spectral correlation function for each detector is calculated. A direct comparison of the normalized correlation function for the two different disorder configurations is shown in fig.3(c). For complete disorder configuration, half-width at half-maxima (HWHM) of the correlation function is $\delta\lambda = 0.70$ nm which is slightly lower compare to half-width at half-maxima $\delta\lambda = 0.80$ nm of periodic disorder configuration.

4. CONCLUSION

We have designed, simulated and fabricated a disorder enhanced photonic-crystal based compact spectrometer to achieve high sensitivity and resolution. With combination of experiment and numerical simulation we shows that for almost identical spectral resolutions, out-of-plane scattering is reduced by 30 % for a disorder enhanced-periodic crystal structure compared to complete random structure for the same scatterer density, paving the way towards high throughput and high-signal to noise ration integrated spectrometers.

ACKNOWLEDGMENTS

This work is funded by EPSRC project EP/V029975/1: "DIsorder enhanced on-chip spectrometers."

REFERENCES

[1] K. A. Willets and R. P. Van Duyne, "Localized surface plasmon resonance spectroscopy and sensing," Annual Review of Physical Chemistry, **58**: 267–297 (2007).

[2] P. A. Martin, "Near-infrared diode laser spectroscopy in chemical process and environmental air monitoring," Chemical Society Reviews, **31(4)**, 201–210.(2002).

[3] T. Matsumoto, S. Fujita, and T. Baba, "Wavelength demultiplexer consisting of photonic crystal superprism and superlens," Optics Express, 2005, **13(26)** 10768–10776, (2005).

[4] S. Janz, A. Balakrishnan, S. Charbonneau, P. Cheben, M. Cloutier, A. Delage, K. Dossou, L. Erickson, M. Gao, P. A. Krug, B. Lamontagne, M. Packirisamy, M. Pearson, D. Xu,"Reflective arrayed waveguide grating with parallel arms using one-dimensional photonic crystal reflector " IEEE Photonics Technol. Lett. 2004, 16, 503.

[5] J.-J. He, B. Lamontagne, A. Delage, L. Erickson, M. Davies, E. S. Koteles, " Waveguide integrated GaN distributed Bragg reflector cavity using low-cost nanolithography " J. Lightwave Technol. 1998, 16, 631.

[6] P. Cheben, J. H. Schmid, A. Delâge, A. Densmore, S. Janz, B. Lamontagne, J. Lapointe, E. Post, P. Waldron, D.-X. Xu, "A high-resolution silicon-on-insulator arrayed waveguide grating microspectrometer with sub-micrometer aperture waveguides " Opt. Express 2007, 15, 2299.

[7] T. Fukazawa, F. Ohno, T. Baba, Jpn. "Very Compact Arrayed-Waveguide-Grating Demultiplexer Using Si Photonic Wire Waveguides " J. Appl. Phys., 43, L673 (2004).

[8] L. P. Schuler, J. S. Milne, J. M. Dell, L. Faraone, J. Phys. D, " MEMS-based microspectrometer technologies for NIR and MIR wavelengths, "Appl. Phys. **42**, 133001 (2009).

[9] B. Mortada, M. Erfan, M. Medhat, Y. M. Sabry, B. Saadany, D. Khalil, "Wideband Optical MEMS Interferometer Enabled by Multimode Interference Waveguides " J. Lightwave Technol. 2016, **34**, 2145 (2016)

[10] N. P. Ayerden, U. Aygun, S. T. S. Holmstrom, S. Olcer, B. Can, J.-L. Stehle, H. Urey, "High-speed broadband FTIR system using MEMS" Appl. Opt., **53**, 7267 (2014).

[11] P. Varytis, D.-N. Huynh, W. Hartmann, W. Pernice, K. Busch, "Design study of random spectrometer for applications at optical wavelengths " Opt. Lett. bf 43, 3180(2018).

[12] W. Hartmann, P. Varytis, H. Gehring, et al.., "Waveguide-integrated broadband spectrometer based on tailored disorder," Adv. Opt. Mater., vol. 8, p. 1901602, 2020,

[13] Redding, B., Liew, S., Sarma, R. et al. "Compact spectrometer based on a disordered photonic chip." Nature Photon **7**, 746–751 (2013).

[14] J. P. Vasco and S. Hughes, "Exploiting Long-Range Disorder in Slow-Light Photonic Crystal Waveguides: Anderson Localization and Ultrahigh Q/V Cavities ACS Photonics", **6(11)**, 2926-2932(2019).

[15] L. O'Faolain, S. A. Schulz, D. M. Beggs, T. P. White, M. Spasenović, L. Kuipers, F. Morichetti, A. Melloni, S. Mazoyer, J. P. Hugonin, P. Lalanne, and T. F. Krauss, "Loss engineered slow light waveguides," Opt. Express **18**, 27627-27638 (2010)

[16] Juntao Li, Liam O'Faolain, Sebastian A. Schulz, Thomas F. Krauss, "Low loss propagation in slow light photonic crystal waveguides at group indices up to 60." Photonics and Nanostructures - Fundamentals and Applications,10,4,2012,589-593,